J|A|C|S
ARTICLES
Published on Web 05/10/2007

Transient Dimerization and Conformational Change of a BLUF Protein: YcgF

Yusuke Nakasone,[†] Taka-aki Ono,[‡] Asako Ishii,[§] Shinji Masuda,[||] and Masahide Terazima*,[†]

Contribution from the Department of Chemistry, Graduate School of Science, Kyoto University, Kyoto, 606-8502, Japan, Department of Biomolecular Functional Engineering, Faculty of Engineering, Ibaraki University, Ibaraki, 316-8511, Japan, Toin Human Science and Technology Center, Toin University of Yokohama, 1614 Kurogane-cho, Aoba-ku, Yokohama, 225-8502, Japan, and Graduate School of Bioscience and Biotechnology, Tokyo Institute of Technology, Yokohama 226-8501, Japan

Received August 5, 2006; Revised Manuscript Received April 3, 2007; E-mail: mterazima@kuchem.kyoto-u.ac.jp

Abstract: The photochemical reaction dynamics of YcgF, a BLUF protein, were investigated by the pulsed laser-induced transient grating (TG) technique. The TG signal showed three reaction time constants: 2.7 μs, 13 μs, and 2 ms. The fastest was tentatively attributed to relaxation of the excited triplet state of the chromophore, flavin adenine dinucleotide (FAD), and the others represented conformational changes of the protein. The TG signal provided clear evidence that the diffusion coefficient (D) of the photoproduct (3.8×10^{-11} m^2 s^{-1}) was significantly less than that of the reactant (8.3×10^{-11} m^2 s^{-1}), with a time constant of 2 ms at a protein concentration of 700 μM. Interestingly, the rate constant increased in proportion to the concentration of the protein, indicating that protein dimerization was one of the main reactions occurring after photoexcitation. The significant reduction in D indicates that a conformational change leading to an increase in interactions with water molecules occurs upon formation of the signaling state. The 13 μs dynamics was attributed to the conformational change that induced transient dimerization. This conformational change might be an essential process for the creation of the signaling state. A detailed scheme for the photochemical reaction of YcgF is proposed.

1. Introduction

BLUF [sensors of *b*lue *l*ight *u*sing *F*AD (flavin adenine dinucleotide)] proteins represent the third class of flavin-containing blue-light receptors together with phototropins (phot) and cryptochromes. They are widespread among prokaryotic and eukaryotic microorganisms[1,2]and include AppA,[3,4] Slr1694,[5] PAC,[6] Tll0078,[7,8] and BlrB,[9] which retain one or more copies of the BLUF domain. It has been shown that the photochemistry of these BLUF domains has a common feature; i.e., signaling state formation is accompanied by a red shift of the UV−visible absorption spectrum.[3,5,7,9,10] FTIR spectroscopic studies and a crystal structure of AppA have shown that hydrogen-bond rearrangement around FAD occurred upon photoexcitation.[11−13] Ultrafast spectroscopy of the BLUF domain of AppA and Slr1694 indicated that transient electron and proton transfer from the protein to FAD took place in a singlet excited state, resulting in a switching of the hydrogen bond network to form the red-shifted state within 1 ns.[7,14,15]

In general, the signal-receiving states of the BLUF domains should communicate the light signal to effector modules, which reside on the same polypeptide chain or another interacting protein, through structural changes in the BLUF domain.[2] Although the photochemistry underlying the activation of intra- or intermolecular receptor domains and, thus, the signal trans-

[†] Kyoto University.
[‡] Ibaraki University.
[§] Toin University of Yokohama.
[||] Tokyo Institute of Technology.

(1) van der Horst, M. A.; Hellingwerf, K. J. *Acc. Chem. Res.* **2004**, *37*, 13−20.
(2) Gomelsky, M.; Klug, G. *Trends Biochem. Sci.* **2002**, *27*, 497−500.
(3) Masuda, S.; Bauer, C. E. *Cell* **2002**, *110*, 613−623.
(4) Braatsch, S.; Gomelsky, M.; Kuphal S.; Klug, G. *Mol. Microbiol.* **2002**, *45*, 827−836.
(5) Masuda, S.; Hasegawa, K.; Ishii, A.; Ono, T. *Biochemistry* **2004**, *43*, 5304−5313.
(6) Iseki, M.; Matsunaga, S.; Murakami, A.; Ohno, K.; Shiga, K.; Yoshida, K.; Sugai, M.; Takahashi, T.; Hori, T.; Watanabe, M. *Nature* **2002**, *415*, 1047−1051.
(7) Fukushima, Y.; Okajima, K.; Shibata, Y.; Ikeuchi, M.; Itoh, S. *Biochemistry* **2005**, *44*, 5149−5158.
(8) Kita, A.; Okajima, K.; Morimoto, Y.; Ikeuchi, M.; Miki, K. *J. Mol. Biol.* **2005**, *349*, 1−9.
(9) Jung, A.; Domratcheva, T.; Tarutina, M.; Wu, Q.; Ko, W. H.; Shoeman, R. L.; Gomelsky, M.; Gardner, K. H.; Schlichting, L. *Proc. Natl. Acad. Sci. U.S.A.* **2005**, *102*, 12350−12355.
(10) Ito, S.; Murakami, A.; Sato, K.; Nishina, Y.; Shiga, K.; Takahashi, T.; Higashi, S.; Iseki, M.; Watanabe, M. *Photochem. Photobiol. Sci.* **2005**, *4*, 762−769.
(11) Masuda, S.; Hasegawa, K.; Ono, T. *Biochemistry* **2005**, *44*, 1215−1224.
(12) Anderson, S.; Dragnea, V.; Masuda, S.; Ybe, J.; Moffat, K.; Bauer, C.E. *Biochemistry* **2005**, *44*, 7998−8005.
(13) Jung, A.; Reinstein, J.; Domratcheva, T.; Shoeman, R. L.; Schlichting, I. *J. Mol. Biol.* **2006,** *362*, 717−32.
(14) Gauden, M.; Yeremenko, S.; Laan, W.; van Stokkum, I. H.; Ihalainen, J. A.; van Grondelle, R.; Hellingwerf, K. J.; Kennis, J. T. *Biochemistry* **2005**, *44*, 3653−3662.
(15) Gauden, M.; Ihalainen, J. A.; Key, J. M.; Luhrs, D. Ch.; van Grondelle, R.; Hegemann, P.; Kennis, J. T. *Proc. Natl. Acad. Sci. U.S.A.* **2006**, *103*, 10895−10900.

 10.1021/ja065682q CCC: $37.00

duction processes have been the focus of much research attention, the photochemistry of BLUF proteins has not been understood well. In particular, because it has been difficult to prepare intact AppA, the photochemistry of solely the BLUF domain of AppA has mainly been studied so far.[11,14] Therefore, intact YcgF provides a valuable opportunity to study the photochemical reaction of an intact BLUF protein.

The YcgF protein from *Escherichia coli* is composed of an N-terminal BLUF domain and a C-terminal EAL domain, which contains an abundance of the amino acids, glutamine (E), alanine (A), and leucine (L).[16,17] The EAL domain has been shown to encode the enzymatic activity involved in the hydrolysis of cyclic diguanosine monophosphate (c-di-GMP), which is a regulatory signaling molecule for various biological events. Therefore, it has been proposed that YcgF functions as a blue-light regulated phosphodiesterase (Blrp).[16] Upon illumination, YcgF exhibits the red-shifted UV−visible absorption of FAD, and this state relaxes to the ground state with a half-dacay time of about 2 min.[18] The formation of the red-shifted species is similar to that of the other BLUF domains.[7,14,15] CD measurements on YcgF showed that no major changes were induced in the secondary structure upon formation of the signaling state.[16] Light-induced structural changes in the YcgF protein were detected using light-induced FTIR difference spectroscopy.[18] However, the nature of the signaling state and the dynamics of the creation of the YcgF signaling state have not been elucidated yet.

In this study, the photoreaction dynamics of YcgF were examined by using the pulsed laser-induced transient grating (TG) method. After the photoexcitation of YcgF, several spectrally silent reaction intermediates were discovered upon examination of changes in volume change and molecular diffusion. A significant observation was the drastic reduction in the diffusion coefficient (D) with a time constant of 2 ms at a concentration of 700 μM. Interestingly, this rate constant increased in proportion to the concentration of the protein. The time dependence of D was attributed to the dimerization of YcgF. It is suggested that the conformational change causing the dimer formation occurred with a time constant of 13 μs. The conformational change of YcgF upon photoexcitation is discussed.

2. Experimental Section

YcgF expressed in *E. coli* was prepared using the method described previously.[18] The protein was purified using a His-Bind resin (Novagen), and dialyzed against a buffer containing 2 mM NaCl, 2 mM $MgCl_2$, and 20 mM Tris/HCl (pH 8.0). The purified protein was dissolved in an aqueous medium containing 20 mM Tris/HCl (DCl), 2 mM NaCl, and 2 mM $MgCl_2$ (pH/pD 8.0) and then stored at −80 °C until use. The concentration of YcgF for most experiments was 700 μM unless otherwise noted. Protein concentrations were determined from the absorbance at 450 nm using the absorption coefficient of FAD (11.3 mM^{-1} cm^{-1}).

The TG measurements were performed using a setup similar to that reported before.[19−27] A pulsed laser with a wavelength of 465 nm was used for a pump beam, and a continuous wave laser with a wavelength of 835 nm was used for a probe beam. The excitation laser beam was divided into two by a beam splitter, and the beams were crossed inside a quartz sample cell (optical path length = 2 mm). The laser power of the excitation was <10 μJ/pulse. The grating wavenumber q was controlled by changing the crossing angle of the two excitation beams. The sample solution was stirred by a magnetic stirrer after every photoexcitation to refresh the sample solutions in the photoexcited area, which was approximately 1 mm^2. The repetition rate of the photoexcitation was 0.01 Hz. Bromocresol purple in aqueous solution was used for the calorimetric reference (CR) sample. For covering a wide time range (10 ns−2.5 s), signals were recorded in several time ranges by a digital oscilloscope and connected into one curve by a computer. At each time range, an appropriate time constant was used by selecting an appropriate external resistance. We were extremely careful not to distort the signal by this instrumental time response in the observation time window.

3. Principles

The principles of TG measurements and analysis of the signal based on a time-dependent D have been reported previously.[19,23−27] Briefly, photoexcitation by sinusoidal modulated light intensity leads to a sinusoidal modulated refractive index (δn) by several processes. This modulation is monitored by the diffraction of a probe beam (TG signal). In this experiment, δn mainly comes from the released thermal energy (thermal grating, $\delta n_{th}(t)$), change in absorption spectrum (population grating), and change in molecular volume (volume grating). The sum of the population grating and volume grating terms is called the species grating ($\delta n_{spe}(t)$). The species grating signal intensity is given by the difference between δn due to the reactant (δn_R) and product (δn_P). The observed TG signal ($I_{TG}(t)$) is expressed as

$$I_{TG}(t) = \alpha\{\delta n_{th}(t) + \delta n_{spe}(t)\}^2 = \alpha\{\delta n_{th}(t) + \delta n_P(t) - \delta n_R(t)\}^2 \quad (1)$$

where α is a constant. The "product" in this equation does not necessarily mean the final product but can be any molecule produced from the reactant at the time of observation. The sign of the $\delta n_R(>0)$ term is negative, because the depletion of the reactant causes the spatial concentration modulation of the reactant to be phase-shifted 180° from that of the product.

The refractive index change due to volume change (δn_v) is given by[19]

$$\delta n_v = V(\mathrm{d}n/\mathrm{d}V)\Delta V \Delta N \quad (2)$$

where $V\mathrm{d}n/\mathrm{d}V$ is the refractive index change by the molecular volume change. By taking the ratio of δn_v to δn_{th} of a CR sample with a known solvent property ($V\mathrm{d}n/\mathrm{d}V$), ΔV was determined from the signal intensity.[19]

(16) Rajagopal, S.; Key, J. M.; Purcell, E. B.; Boerema, D. J.; Moffat, K. *Photochem. Photobiol.* **2004**, *80*, 542−547.
(17) Masuda, S.; Ono, T. In *Photosynthesis: Fundamental Aspects to Global Perspectives*; van der Est., A., Bruce, D., Eds.; Allen Press: Lawrence, KS, 2005; Vol. II, pp 700−702.
(18) Hasegawa, K.; Masuda, S.; Ono, T. *Biochemistry* **2006**, *45*, 3785−3793.
(19) Inoue, K.; Sasaki, J.; Morisaki, M.; Tokunaga, F.; Terazima, M. *Biophys. J.* **2004**, *87*, 2587−2597.
(20) Terazima, M.; Okamoto, K.; Hirota, N. *J. Chem. Phys.* **1995**, *102*, 2506−2512. Khan, J. S.; Imamoto, Y.; Kataoka, M.; Tokunaga, F.; Terazima, M. *J. Am. Chem. Soc.* **2006**, *128*, 1002−1008.
(21) Terazima M. *Acc. Chem. Res*. **2000**, *33*,687−694.
(22) Nada, T.; Terazima, M. *Biophys. J.* **2003**, *85*, 1876−1881.
(23) Nishida, S.; Nada, T.; Terazima, M. *Biophys. J.* **2004**, *87*, 2663−2675.
(24) Eitoku, T.; Nakasone, Y.; Matsuoka, D.; Tokutomi, S.; Terazima, M. *J. Am. Chem. Soc.* **2005**, *127*, 13238−13244.
(25) Terazima, M. *Phys. Chem. Chem. Phys.*, **2006**, *8*, 545-557.
(26) Hazra, P.; Inoue, K.; Laan, W.; Hellingwerf, K, J.; Terazima, M. *Biophys. J.* **2006,** *91*, 654−661.
(27) Nakasone, Y.; Eitoku, T.; Matsuoka, D.; Tokutomi, S.; Terazima, M.; *Biophys. J.* **2006,** *91*, 645−653.

The temporal profiles of the thermal grating and the species grating can be calculated by diffusion equations. The thermal grating, $\delta n_{th}(t)$, decays with a rate constant of $D_{th}q^2$,

$$\delta n_{th}(t) = \delta n_{th}^0 \exp(-D_{th}q^2 t)$$

where δn_{th}^0 is the initial refractive index change of the thermal grating, D_{th} is the thermal diffusivity, and q is the grating wavenumber.[19−27]

When the molecular diffusion coefficient (D) is time-independent, the temporal profile of the species grating signal can be calculated by the molecular diffusion equation. The q-Fourier component of the concentration decays with a rate constant Dq^2 for the reactant and the product. Hence, the time development of the TG signal can be expressed by[19−21]

$$I_{TG}(t) = \alpha\{\delta n_P^0 \exp(-D_P q^2 t) - \delta n_R^0 \exp(-D_R q^2 t)\}^2 \quad (3)$$

where D_R and D_P are diffusion coefficients of the reactant and the product, respectively. Furthermore, $\delta n_R^0(>0)$ and $\delta n_P^0(>0)$ are, respectively, the initial refractive index changes due to changes in reactant and product concentrations during the reaction.

When the apparent D is time dependent, the observed TG signal should be calculated from a diffusion equation with a concentration-dependent term. Describing the reaction by the following two-state model,

$$R \xrightarrow{h\nu} I \xrightarrow{k} P$$

where R, I, P, and k represent, respectively, a reactant, an intermediate species, a final product, and the rate constant of the change, one may find the time-dependence of the refractive index as[20,22−24]

$$\delta n_P(t) = \delta n_I^0 \exp(-(D_I q^2 + k)t) + \frac{\delta n_P^0 k}{(D_P - D_I)q^2 - k}\{\exp(-(D_I q^2 + k)t) - \exp(-D_P q^2 t)\}$$

$$\delta n_P(t) = \delta n_R^0 \exp(-D_R q^2 t) \quad (4)$$

where δn_I and D_I are the refractive index change due to the formation of the intermediate species and the diffusion coefficient of the intermediate species, respectively. Here, it should be noted that $\delta n_P(t)$ describes the species grating signal of the product as well as the intermediate, both of which are created by the photoexcitation of the reactant.

4. Results and Discussion

4.1. Photoinduced Reactions. A typical TG signal YcgF in the buffer solution at 700 μM with $q^2 = 2.3 \times 10^{13}$ m^{-2} is shown in Figure 1. Immediately after excitation, the signal rose quickly with the time response of our system (~20 ns). After this, the signal initially decayed and then was followed by two rise−decay components before finally decaying to the baseline. The initial decay−rise components could be expressed by a single-exponential function with a subsequent slower component $\delta n_{spe}(t)$. This rate constant agreed well with $D_{th}q^2$ determined from a signal of the CR sample. Therefore, this signal could be attributed to the thermal grating component:

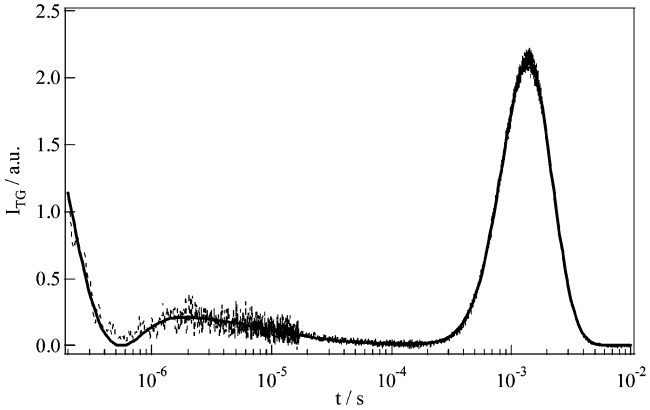

Figure 1. Typical TG signal (broken line) after photoexcitation of full-length YcgF at a concentration of 700 μM at $q^2 = 2.3 \times 10^{13}$ m^{-2}. The best-fit curve based on the two-state model (eqs 1 and 4) is shown by the solid line.

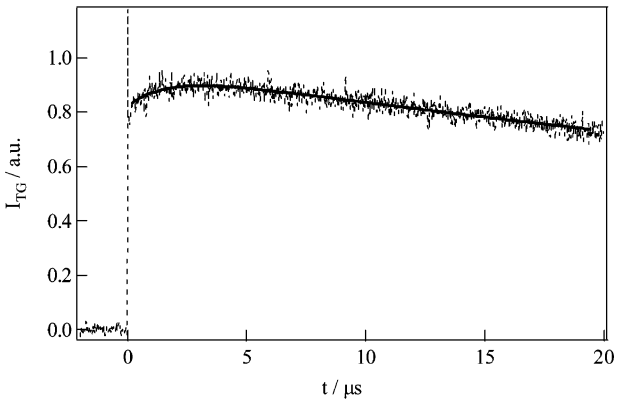

Figure 2. Initial part of the TG signal (broken line) observed at 700 μM and at $q^2 = 5.7 \times 10^{10}$ m^{-2}. The best-fit curve based on a single-exponential function with the thermal grating component is shown by the solid line.

$$I_{TG}(t) = \alpha\{\delta n_{th}^0 \exp(-D_{th}q^2 t) + \delta n_{spe}(t)\}^2 \quad (5)$$

The decay−rise feature around 500 ns in Figure 1 arose due to the cancellation between this thermal grating contribution and the species grating contribution.

Figure 2 depicts the rising part of the thermal grating signal at a small q^2 ($q^2 = 5.7 \times 10^{10}$ m^{-2}). At this small q^2, the decay of the thermal grating signal was much slower than that of Figure 1, so that a weakly rising component was clearly observed. (The weak decay component observed in Figure 1 in a few microsecond time range was not obvious in this signal, because a relatively strong thermal grating signal masked this component.) The time constant of this slow rise was determined to be 2.7 μs from a single-exponential fit with the thermal grating component. This time constant was independent of q^2, indicating that this component represented the reaction kinetics of the protein, not a diffusion process. The calculated time constant was close to the reported triplet lifetime of FAD (3 μs) in AppA,[14] another BLUF protein. Hence, the 2.7 μs kinetics was tentatively attributed to the decay of the triplet state of FAD in YcgF. The species grating may have been composed of the volume grating due to the volume change of the protein and the population grating due to the absorption change of the

chromophore FAD.[28,29] The exact assignment and characterization of this component is not a subject in this paper, and the details have been left for future examination.

The thermal grating signal was followed by a decay component that could be fitted by a single-exponential function with a time constant of 13 μs (Figure 1). This decay cannot be due to the heat releasing, because this component was observed at a large q^2 (Figure 1), at which the thermal grating component should be very weak due to the rapid thermal diffusion process.[20] Since the rate of this decay was independent of q^2, this component was attributed to an intrinsic dynamics of the protein. Furthermore, since there was no absorption change accompanying this process, the origin of this signal cannot be the population grating, but it was assigned to the volume grating.

The time range in which the last rise−decay signal appeared increased with decreasing q^2. This q^2-dependence indicated that this peak represented molecular diffusion processes (i.e., diffusion peak). Therefore, writing the diffusion contribution as $\delta n_P(t) - \delta n_R(t)$, the TG signal profile could be expressed by the following equation:

$$I_{TG}(t) = \alpha\{\delta n_{th}^0 \exp(-D_{th}q^2t) + \delta n_1 \exp(-t/\tau_1) + \delta n_P(t) - \delta n_R(t)\}^2 \quad (6)$$

where the $\delta n_1 \exp(-t/\tau_1)$ term represents the 13 μs dynamics. The sign of the thermal grating at this temperature is negative ($\delta n_{th}^0 < 0$). Hence, the dip reaching to the baseline in Figure 1 (at ~500 ns) indicated that the sign of the refractive index change was changed from negative to positive at this time. Based on this fact, the sign of δn_1 was determined to be positive. Similarly, the refractive index (δn) of the later rise and decay components were determined to be negative and positive, respectively. By comparing with eq 1 or 6, the rise and decay components were readily attributed to the diffusion of the reactant [$\delta n_R(t)$] and the product [$\delta n_P(t)$], respectively.[20,21] This assignment indicated that the product diffused more slowly than the reactant. The origin of the slower diffusion of the product will be discussed in a later section.

4.2. Time-Dependent Diffusion Coefficient. The rise−decay profile of the diffusion signal was a clear indication that the product and reactant had different values of D.[20,21] It was important to determine when D of the product became different from that of the reactant. Since D is a physical property representing the conformation of the protein, this kinetic information is needed to understand the reaction. If D of YcgF changed quickly (<100 μs) by the photoexcitation and did not change any more, it should be possible to express the profile of molecular diffusion by a biexponential function (eq 3). However, although we have tried to fit the data after the decay of the thermal grating signal by a biexponential function, the profile cannot be reproduced well (Figure 3). This feature was therefore interpreted in terms of time-dependent changes in D for the following reasons.

First, if any D changes could be neglected during the diffusion process, the time-dependence should have been expressed by a combination of $\exp(-Dq^2t)$ terms (e.g., eq 3). In this case, if the signals are plotted against q^2t, the shape of the signals at various q^2 would be identical. However, it changed significantly depending on q^2 (Figure 4). Therefore, we concluded that D changed in a time-dependent manner during this observation time range. Second, we found that the species grating signal intensity depended on q^2 (Figure 5). If any reaction dynamics were complete before the diffusion peak, the species grating signal intensity would not depend on q^2. Contrary to this

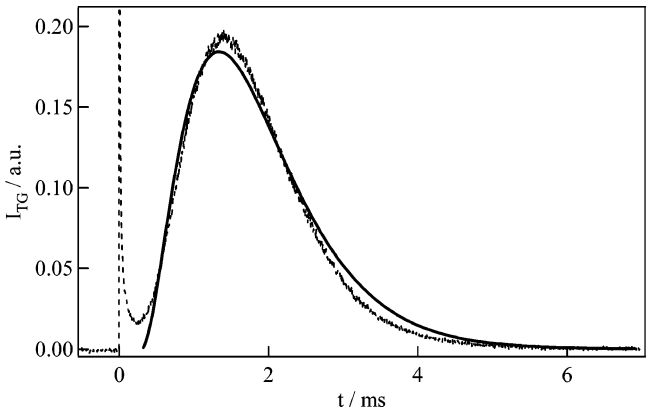

Figure 3. A typical TG signal (broken line) of YcgF at a concentration of 700 μM with $q^2 = 2.3 \times 10^{13}$ m^{-2}. The signal cannot be reproduced by the biexponential function of eq 3 (solid line).

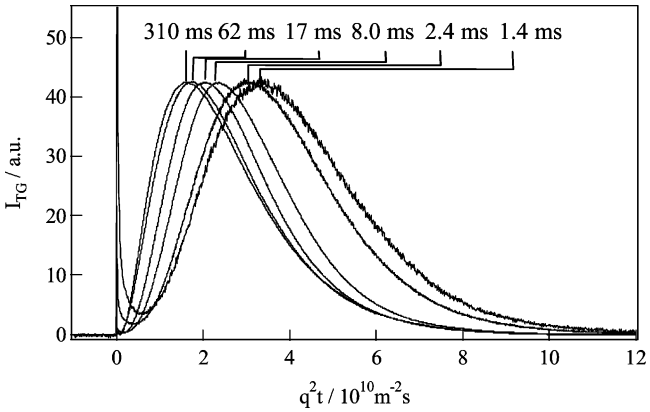

Figure 4. TG signals of YcgF at 700 μM plotted against q^2t to show the time dependence of D. The q^2 values were 2300, 1300, 290, 120, 27, 5.7 $\times 10^{10}$ m^{-2}. The times of the peaks are shown in the figure.

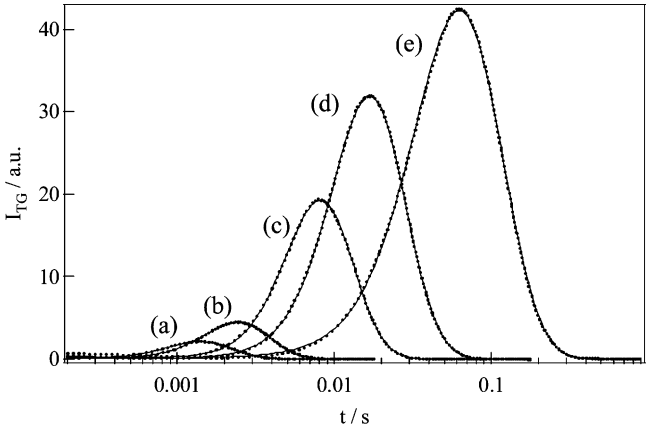

Figure 5. q^2-dependence of the TG signal (dotted line) of YcgF at 700 μM. The q^2-values were (a) 2.3×10^{13}, (b) 1.3×10^{13}, (c) 2.9×10^{12}, (d) 1.2×10^{12}, and (e) 2.7×10^{11} m^{-2}. The signals were normalized by the thermal grating intensity measured under the same condition (not seen in this time range). The best-fit curves obtained from the two-state model are shown by the solid lines, which almost completely overlapped the observed signals.

(28) Kennis, J. T. M.; Crosson, S.; Gauden, M.; van Stokkum, I. H. M.; Moffat, K.; van Grondelle, R. *Biochemistry* **2003**, *42*, 3385−3392.
(29) Sakai, M.; Takahashi, H. J. *Mol. Struct.* **1996**, *379*, 9−18.

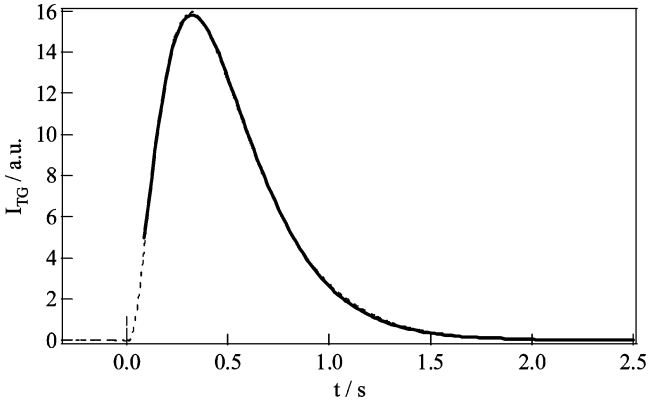

Figure 6. Observed TG signals (broken line) of YcgF at 700 μM at a relatively low q^2 of $q^2 = 5.7 \times 10^{11}$ m^{-2}. This signal could be fitted well by a biexponential function after 100 ms (solid line).

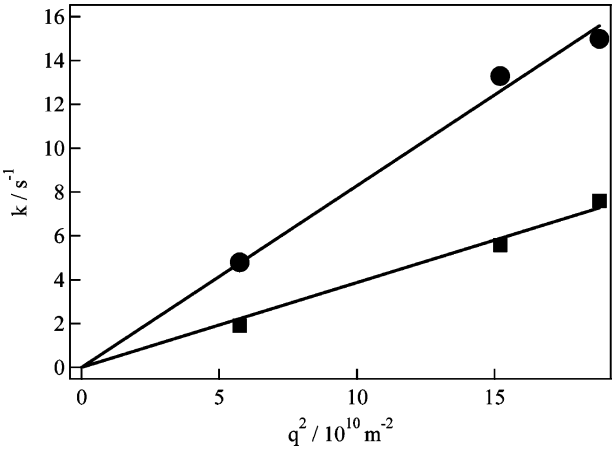

Figure 7. Plot of rate constants of the reactant (circles) and product components (squares) against q^2. The best fitted lines by a linear function ($k = D_i q^2$; i = P and R) are shown by the solid lines.

expectation, the TG signal on a fast time scale was weak and its intensity increased at a longer observation time. This time dependence could be explained using a time-dependent D as follows. Suppose D_p in eq 3 was similar to D_R, the contributions of the two diffusing species would cancel each other and the signal intensity would be weak due to the opposite signs of δn_P and δn_R. With an increasing difference between D_P and D_R, the peak signal intensity would become stronger. Since D_R is constant, the time dependence of the signal intensity must have arisen from the time-dependent decrease in D_P. This feature is similar to the case of the LOV2 domain in phototropin 2 (phot2-LOV2) retaining the linker domain, whose profile was explained by time-dependent diffusion.[24]

The molecular diffusion signal was fitted using the two-state model described in section 3. In order to reduce the number of adjustable parameters in eq 4, D_R and D_P were determined as follows. First, the time range in which the reaction kinetics affected the profiles was roughly estimated from the q^2t plots in Figure 4. The signals plotted against q^2t were similar at low q^2; i.e., D was almost time-independent at times >100 ms. It will be shown below that this time was indeed sufficiently longer than the time constant of this decay. Therefore, the temporal profile after this time was fitted by a biexponential function (eq 3) to determine D_R and D_P. The good fit (Figure 6) confirmed that D did not depend on time after 100 ms.

Figure 7 shows plots of the rate constants for the reactant and product diffusions against q^2. From the slopes, D_R and D_P were determined to be 8.3×10^{-11} m^2 s^{-1} and 3.8×10^{-11} m^2 s^{-1}, respectively. Furthermore, the very weak diffusion signal at large q^2 (Figure 5) suggested that the change in D just after the photoexcitation was very small; that is, $D_R \approx D_I$. Using these values for D, the signals could be reproduced well over the wide time range from 500 μs to 100 ms with a single adjustable kinetic parameter, k, in eq 4 (e.g., Figures 1 and 5). The time constant of the D change was determined to be 2.0 $\pm$ 0.5 ms.

If this D-change process accompanied any conformational change, this change would have been observed in the TG signal as the volume grating component. However, over the range of q^2 normally used (6×10^{11}−4×10^{13} m^{-2}), the TG signal showed a strong diffusion signal (the rise-decay component, e.g., Figure 1), and this strong diffusion signal masked any possible volume grating component. In order to examine a possible volume change process, we measured the TG signal at a much smaller q^2 (<2×10^{11} m^{-2}) so that the diffusion peak was shifted to a longer time range. Theoretically, this method can be explained as follows. The temporal profile of the TG signal would have been expressible by eq 4 and 6. At a very low q^2 ($D_P q^2$, $D_R q^2 < k$ in eq 4), these equations are reduced to

$$I_{TG}(t) = \alpha\{\delta n_{th}^0 \exp(-D_{th}q^2t) + \delta n_1 \exp(-t/\tau_1) + (\delta n_I^0 - \delta n_P^0)\exp(-kt) + \delta n_P^0 \exp(-D_P q^2 t) - \delta n_R^0 \exp(-D_R q^2 t)\}^2 \quad (7)$$

Hence, if ($\delta n_I^0 - \delta n_P^0$) were nonzero, the kinetics of the diffusion change (exp($-kt$)) would have appeared clearly. Since there was no absorption change during this process, this ($\delta n_I^0 - \delta n_P^0$) reflected a volume change. Although this was equivalent to monitoring the time-dependence of the D-change to determine k, it provided us direct information on the volume change.

When the TG signal was measured at small q^2 (1.6×10^{11} m^{-2}), another weak peak was observed before the diffusion peak (Figure 8a and b); i.e., the TG signal following the thermal diffusion reached the baseline twice before the diffusion peak. This profile looks complicated, but it was reproduced well by eq 7. The contributions of the individual exponential terms in the fitting are shown in Figure 8c. It should be noted that the decay−rise curve around 1 ms was described by a single-exponential function with an amplitude of $\delta n_I^0 - \delta n_P^0$. The decay−rise behavior appears, because δn changes its sign from positive to negative at 0.8 ms in Figure 8b and the TG signal is proportional to the square of δn (eq 1).

The rate k was estimated to be 2 $\pm$ 1 ms (Figure 8b), which is reasonably close to the time constant determined from the change in D within experimental error. However, since the intensity of the exp($-kt$) component was weak and partially overlapped the stronger diffusion signal, the rate of this phase determined from this fitting was less reliable. Therefore, we determined k based on the time-dependent D analysis of the diffusion peak as shown above. Since no further absorption change has been reported after the formation of product with

the "red-shifted spectrum" in known BLUF proteins (AppA,[14] Tll0078,[7] and Slr1694[15]), these species grating signals were not due to the population grating and, hence, should be attributed to a volume change of the protein. These volume changes associated with these phases were calculated by the method in section 3 from the amplitudes of the refractive index changes δn_1 and $(\delta n_I^0 - \delta n_P^0)$ to be 3.5 ± 1.5 mL/mol and 7.3 ± 2.0 mL/mol for the first (13 μs) and second (2 ms) phases, respectively.

On the basis of these observations, the following reaction scheme is proposed for 700 μM,

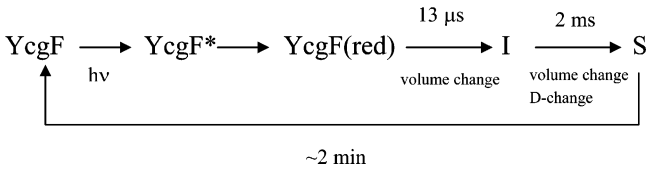

where YcgF*, YcgF(red), I, and S denote the excited singlet state of FAD, the red-shifted state, the intermediate, and the final signaling state, respectively.

It is instructive to compare D_R with D values of other proteins. The molecular weight of full-length YcgF is ~47 kDa. D values for water-soluble proteins with a similar molecular weight, e.g., lectin from *Lens culinaris*[30] (45 − 50 kDa) (7−8) × 10^{-11} m^2/s and ovalbumin[31] (45 kDa) 7.8 × 10^{-11} m^2/s, are close to D_R (=8.3 × 10^{-11} m^2 s^{-1}) for YcgF. Therefore, we consider that YcgF exists in the monomeric form in solution and that protein−protein interactions were negligibly weak in the dark state. Consistent with this, it has been reported that full-length YcgF exists as a monomer in the dark state based on gel chromatography measurements.[16]

4.3. Origin of the Change in *D*. According to the Stokes−Einstein relationship, D is inversely proportional to the radius of a molecule.[32,33] If the difference in D between the reactant and the product (D_R/D_P=2.2) was interpreted only in terms of the difference in molecular radius, the molecular volume of the product would be $(2.2)^3 = 11$ times larger than that of the reactant.[32,33] However, the volume expansion process with 2.0 ms was 7.3 mL/mol, too small to account for the decrease in D.

Alternatively, the reduction in D could be explained by oligomerization (e.g., dimerization) of YcgF or enhancement of the interaction between the protein and water molecules upon illumination. To examine these possibilities, we measured the TG signal at various protein concentrations. If oligomerization was the cause of the reduction in D, the reaction rate should have decreased with decreasing protein concentration. On the other hand, if conformational changes in the protein were responsible for this change, the reaction rate should have been independent of concentration.

We measured the TG signal at various sample concentrations at relatively large q^2, so that the signal profile reflected the kinetics of the change in D. Figure 9 depicts the concentration dependence (from 230 μM to 750 μM) of the TG signals at $q^2 = 2.3 \times 10^{13}$ m^{-2}. When the observed signals were normalized by the thermal grating intensity, which is an indicator of the amount of photoexcited protein (Figure 9a), it was found that the intensity of the diffusion peak decreased with decreasing concentration. Considering that the diffusion signal arose from the difference between D_P and D_R, one may understand that the change in D decreased upon dilution in this time range. When the signals were normalized by the peak intensity of the diffusion signal (Figure 9b), it was clearly seen that the signal shifted to longer times with decreasing concentration. The ground state absorption spectra at these concentrations (Figure 9c) did not show any evidence of aggregation or denaturation that affects the absorption spectrum. This concentration depen-

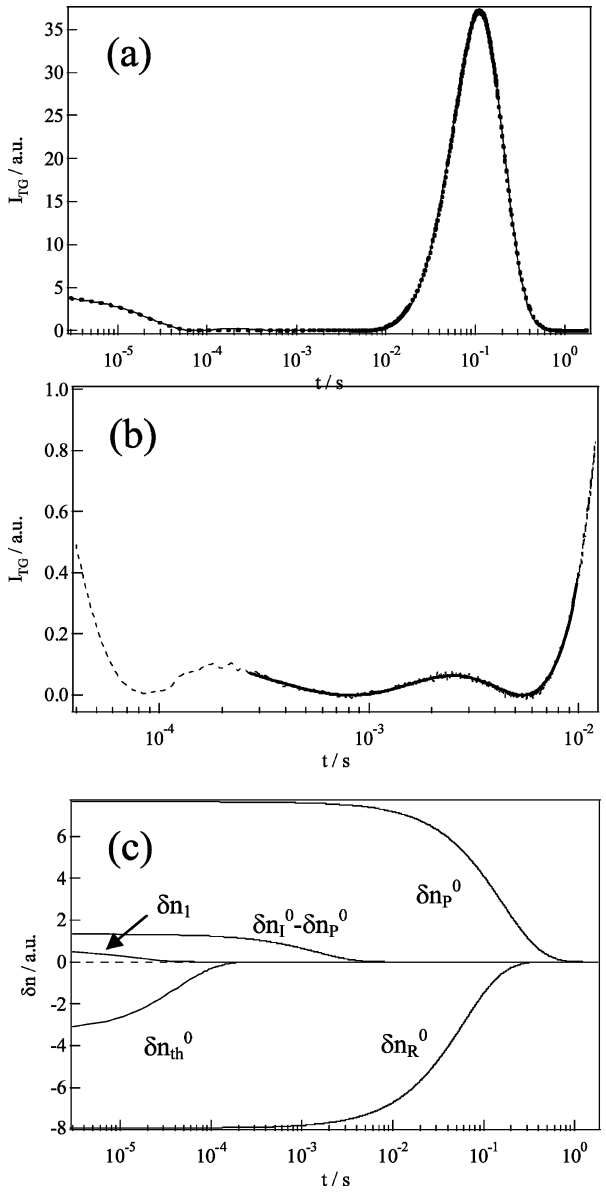

Figure 8. (a) TG signal (dotted line) of YcgF at a concentration of 700 μM at $q^2 = 1.6 \times 10^{11}$ m^{-2}. The best-fit curve based on the two-state model (eqs 1 and 4) is shown by the solid line, which almost completely overlapped the observed signal. (b) The middle time range of (a) has been expanded to show the profile clearly (dotted line). The best-fit line in this time region is shown by the solid line. (c) Schematic decomposition of the components of the TG signal according to eq 7. The intensities of the diffusion components (δn_P^0 and δn_R^0) have been reduced by one-third to show their behavior more clearly. The observed TG signal (a) could be reproduced by taking the square of the sum of these components.

(30) Albani, J. R. *Biochim. Biophys. Acta* **1998,** *1425*, 405−410.
(31) Waheed, A.; Salhuddin, A. *Biochem. J.* **1975,** *147*, 139−44.
(32) Cussler, E. L. *Diffusion*; Cambridge University Press: Cambridge, 1994.
(33) Tyrrell, H. J. V.; Harris, K. R. *Diffusion in liquids*; Butterworth: London, 1984.

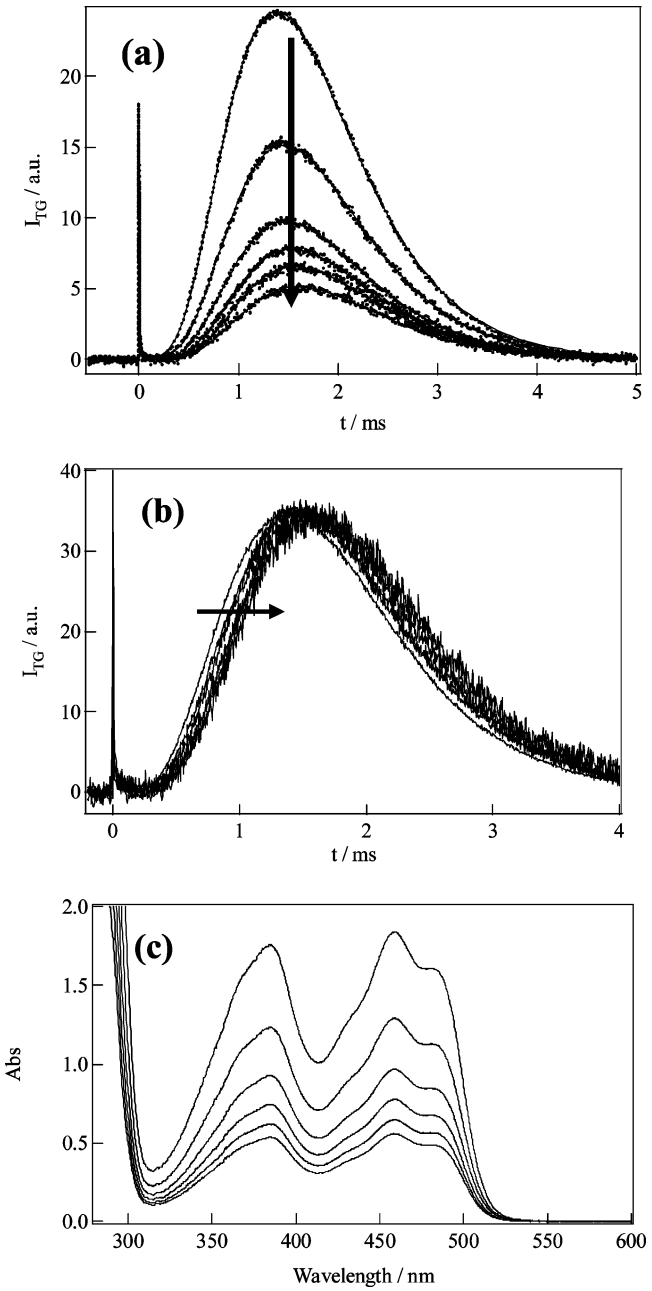

Figure 9. (a) Concentration dependence of the TG signal (dotted lines) at $q^2 = 2.3 \times 10^{13}$ m^{-2} normalized by the intensity of thermal grating signal. (For accurate comparison of the thermal grating signal intensity, the signal at each concentration was also measured in a shorter time range under the same conditions.) The arrow indicates the direction of decreasing concentration. The concentrations were 750, 520, 390, 310, 260, and 230 μM. The best-fit curves are shown by the solid lines, which almost completely overlapped the observed signal. (b) The TG signals of (a) normalized by the peak intensity of the diffusion signal. The arrow indicates the direction of decreasing concentration. (c) Absorption spectra at these concentrations.

dence of the rate was a clear indication that more than one protein molecule was involved in the reaction.

The signals at all concentrations could be reproduced based on the two-state model (Figure 9a), and this agreement strongly implied that an intermediate species (I) was associated with the ground state protein (YcgF) to yield the dimer.

$$\mathrm{I} + \mathrm{YcgF} \xrightarrow{k_{obsd}} (\mathrm{I{\cdot}YcgF})$$

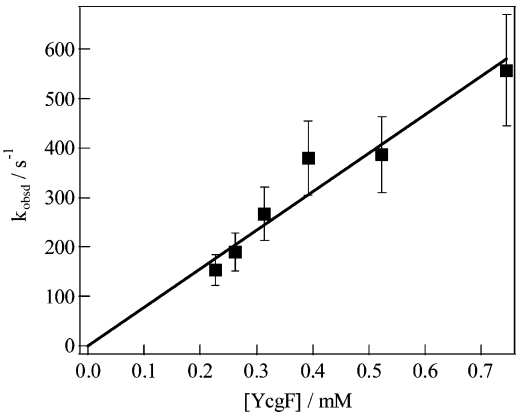

Figure 10. Rate constants (k_{obsd}) obtained from fitting the TG signals at various concentrations of YcgF plotted against YcgF concentration.

On the basis of the above dimerization model, the rate constant k in eq 4 could be seen to correspond to k_{obsd} (i.e., $k_{obsd} = k$). The k_{obsd} determined from the two-state model was plotted against the concentration of YcgF ([YcgF]) in Figure 10. The observed time ranges of the signals in Figure 9 were determined not only by the rate constant of the diffusion change but also by the diffusion rate. Hence, the temporal shift of the signal (Figure 9b) was rather small compared with the concentration dependence of the rate constants. We have fitted the signal to not only the temporal profile but also the signal intensity, and the fitting was almost perfect (Figure 9a). This satisfactory fitting indicated that the rate constant we determined from the signal is reliable.

Since the rate constant was proportional to the concentration, the observed change in D was attributed to a bimolecular reaction, that is, a dimerization process. From the slope of the plot of k_{obsd} versus concentration (Figure 10), the second-order rate constant k_d, which was defined by $k_{obsd} = k_d$[YcgF], was determined to be 7.8×10^5 M^{-1} s^{-1}. This value was much smaller than that of a diffusion-controlled reaction calculated by the Smoluchowski−Einstein equation for a bimolecular reaction in solution ($\sim 10^9$ M^{-1} s^{-1}, using the following parameters: 10 nm as the reaction radius and 1.2×10^{-10} m^2/s as the relative translational diffusion constant).[34] This difference indicated that the collision between two protein molecules was not sufficient for dimerization to occur; i.e., their relative orientations dictated additional constraints, which slowed down the rate of the reaction by 4 orders of magnitude. Furthermore, this small k_d suggested a very small steric factor; that is, the dimerization reaction occurred only at a specific portion of the protein.

It was concluded that the photoinduced dimer eventually dissociated to recover the monomer, because the observed signal was reproducible as long as the repetition rate of the excitation pulse was slow enough (interval between successive light pulses >100 s). Therefore, this dimer was a transient species.

This constitutes the first observation of a transient dimer in YcgF photochemistry. Several proteins exist as oligomers, e.g., a dimer for the BLUF domain of AppA and decamers for T110078 and Slr1694.[8,12,35] These results may indicate that the BLUF proteins tend to undergo attractive intermolecular interac-

(34) Smoluchowski, M. V. *Z. Phys. Chem.* **1997**, *92*, 129−168.
(35) Yuan, H.; Anderson, S.; Masuda, S.; Dragnea, V.; Moffat, K.; Bauer, C. *Biochemistry* **2006**, *45*, 12687−12694.

tions. YcgF itself does not form any oligomers in the ground state, but the observations reported here indicated that the interprotein interactions were enhanced by a conformational change, resulting in the formation of a dimer. It may be reasonable to consider that the kinetics with the time constant of 13 μs represents the conformational change responsible for the dimerization.

4.4. Conformational Change in the Protein Moiety. As mentioned above, if the Stokes−Einstein equation was used, the observed change in *D* could be explained by an 11-fold increase in the molecular volume of the product. However, the partial molar volume approximately doubled as a result of this dimerization reaction, not large enough to account for the change in *D*. Therefore, there must have been another contribution to the difference in *D*. A conformational change in the protein leading to increased interaction between solvent and protein ("diffusion-sensitive conformational change") was considered as a possible explanation. In the case of the LOV2 domain with the linker part of phot2, the photoexcitation caused a decrease in *D* of the product and this was attributed to a strong interaction between the protein and solvent due to unfolding of the α-helix in the linker part.[23] As for the BLUF domain, it has been reported that AppA, T110078, Slr1694, and BlrB consist of two α-helices, between which the FAD chromophore is anchored,[8,12,35,36,37] and some rearrangement of the hydrogen bonding between flavin and conserved residues has been observed after photoexcitation.[5,36] If unfolding of these α-helices was triggered by such a rearrangement of the hydrogen-bonding network and by dimer formation, the interaction between protein and solvent would have strengthened and *D* of the product should have decreased. The conformational change in the EAL domain could be a cause of the diffusion change. We will clarify this point in future by using the BLUF domain without the EAL domain. In any case, such a "diffusion-sensitive conformational change" is the origin of the large observed reduction in *D* of YcgF upon photoexcitation.

Dimerization was accompanied by an increase in the partial molar volume of the protein (ΔV = 7.3 mL/mol). It was speculated that this expansion may come from an increase in void volume upon formation of a hydrophobic bond; that is, the amount of inaccessible space may be increased upon the hydrophobic binding, leading to an increase in the partial molar volume of the protein as detected in this study.

Interestingly, photoinduced aggregation reactions have been reported for some photosensor proteins such as phot1-LOV2 without linker[27] and another BLUF protein, AppA,[26] using diffusion measurements, and also suggested for phytochromes.[38] Although this common feature does not necessarily mean that the dimerization may be essential for the creation of the signaling state, a conformational change that can induce the aggregation process could be important for the signaling state formation of sensor proteins. In some of the previous cases the proteins were not intact, but rather parts of larger proteins, e.g., the LOV2 domain for phot1 and only the BLUF domain for AppA. Here, YcgF provided an opportunity to study the photochemical reaction of an intact BLUF protein. This study is the first example showing the conformational change that can induce dimerization among intact sensor proteins. The reactions derived from this study of YcgF are illustrated schematically in Figure 11.

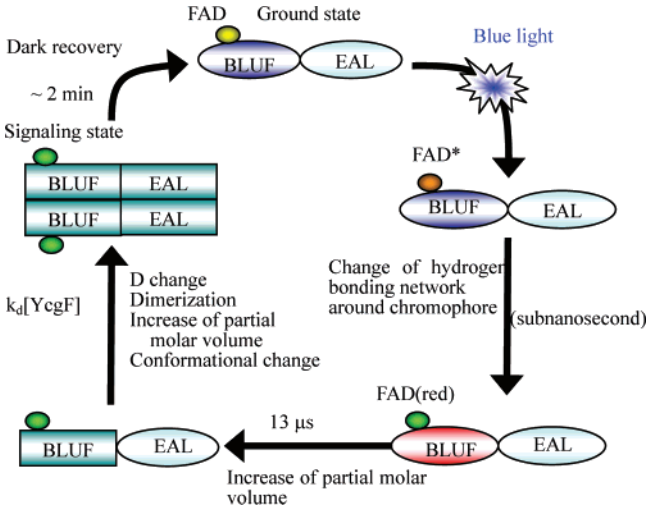

Figure 11. Schematic illustration of the photocycle of intact YcgF. BLUF and EAL denote the BLUF and EAL domains, respectively (FAD*: excited singlet state of FAD).

5. Conclusion

The kinetics of the photoreaction of intact YcgF were studied, with particular attention to its diffusion coefficient (*D*), using the pulsed laser induced transient grating method. It was found that the partial molar volume of YcgF increased with a time constant of 13 μs upon photoexcitation. This should be a spectral silent intermediate that has not been observed before. Furthermore, *D* of YcgF decreased significantly upon photoexcitation from $(8.3 \pm 0.4) \times 10^{-11}$m^2 s^{-1} to $(3.8 \pm 0.3) \times 10^{-11}$ m^2 s^{-1}. Interestingly, *D* of the photoproduct was time-dependent, and the time constant of this change in *D* was determined to be 2 ms at a concentration of 700 μM. Moreover, since the rate of this change depended on the protein concentration, we attributed the change in *D* to a dimerization process. The dimerization rate constant (k_{obsd}) increased as the concentration increased, and from the plot of k_{obsd} against the concentration, the second-order rate constant was determined to be ca. 7.8×10^5 M^{-1} s^{-1}. This value was much smaller than the predicted diffusion-controlled rate and attributed to the orientational constraints on YcgF during dimer formation. The magnitude of the change in *D* suggests that there is another contribution besides the volume change for the observed *D*-change (diffusion-sensitive conformational change) and is attributed to the change of the intermolecular interaction caused by the conformational change upon the formation of the signaling state. This diffusion-sensitive conformational change might be an essential process for the creation of the signaling state.

Acknowledgment. This work was supported by the Grant-in-Aid (Nos. 13853002 and 15076204) from the Ministry of Education, Science, Sports and Culture in Japan.

JA065682Q

(36) Han, Y.; Braatsch, S.; Osterloh, L.; Klug, G. *Proc. Natl. Acad. Sci. U.S.A.* **2005**, *101*, 12306−12311.
(37) Unno, M.; Sano, R.; Masuda, S.; Ono, T.; Yamauchi, S. *J. Phys. Chem. B* **2005**, *109*, 12620−12626.
(38) Rockwell, N. C.; Su, Y.-S.; Lagarias, J. C. *Annu. Rev. Plant Biol.* **2006**, *57*, 837−858.